The Role of Irrigation in Determining the Global Land Use Impacts of Biofuels

By

Farzad Taheripour, Thomas W. Hertel, and Jing Liu

Authors Affiliation
Farzad Taheripour is energy economist, Thomas W. Hertel is distinguished professors, and Jing Liu is Ph.D. Student in the Department of Agricultural Economics at Purdue University.

Corresponding Author
Farzad Taheripour
Department of Agricultural Economics
Purdue University
403 West State St.
West Lafayette, IN 47907-2056
765-494-4612
Fax 765-494-9176
E-mail: tfarzad@purdue.edu

Selected Paper prepared for presentation at the Agricultural & Applied Economics Association's 2011 AAEA & NAREA Joint Annual Meeting, Pittsburgh, Pennsylvania, July 24-26, 2011

The Role of Irrigation in Determining the Global Land Use Impacts of Biofuels

Farzad Taheripour, Thomas Hertel, and Jing Liu

Abstract

In recent years there has been a flurry of activity aimed at evaluating the land use consequences of biofuels programs and the associated carbon releases. In this paper we argue that these studies have tended to underestimate the ensuing land use change, because they have ignored the role of irrigation, and associated constraints on cropland expansion. In this paper, we develop a new general equilibrium model which distinguishes irrigated and rainfed cropping industries at a global scale. Using the new model we evaluate the implications of land use change due to US ethanol programs, in the context of short run constraints on the expansion of irrigated cropland. Since irrigated area tends to offer a higher yield than its rainfed counterpart, this provides an upper bound on the change in cropland following biofuel expansion. We find that the biofuel-induced expansion in global cropland cover is about 16 percent larger when the irrigation constraint is imposed. This translates into a 21 percent increase in land use emissions due to US ethanol production. This estimate represents an upper bound, since irrigated area can be expanded over the medium run in many places around the world.

1. Introduction

Previous research into the global land use impacts of biofuels has assumed that cropland area could expand in most regions of the world. Such estimated expansion into more carbon-rich land cover such as grassland or forest is the focus of recent research into the contributions of indirect land use changes (ILUC) to the GHG impacts of biofuels. Several studies have examined the global land use consequences of biofuel production (e.g. Gurgel et al., 2007; Searchinger, et al., 2008; Hertel et al., 2010, Taheripour et al., 2010, and Tyner et al. 2010). However, all of these studies have effectively treated all cropland as being rainfed. The role of irrigation in biofuel-induced cropland expansion has been wholly ignored. This could introduce systematic diminishing biases in measuring indirect land use emissions due to production of biofuels.

Irrigated croplands typically have much higher yields than their rainfed counterparts in the same Agro Ecological Zone (AEZ). Thus, the question of whether expansion of global cropland cover involves irrigated or rainfed lands makes a significant difference in terms of how much new land will be required to provide the additional production called for in the presence of biofuels. If the new lands are irrigated, and therefore have higher yields than rainfed lands in the same AEZ, then less land conversion will be required. However, if expansion of irrigated area is constrained, either due to insufficient water, or due to insufficient capacity, then the answer could be quite different. In general, if expansion of irrigation is constrained anywhere in the world, it is likely that more cropland area will be required to meet the additional global demand induced by ethanol production.

A recent report by McKinsey & Co (2009), offers an assessment of water availability over the coming two decades, drawing heavily on the IFPRI water model (Cai and Rosegrant, 2002). They start at the river basin level and calculate water demand based on current technology

and expected growth in agricultural and industrial output as well as population. In the absence of efficiency gains, they estimate that water demand will exceed existing sustainable, reliable water supply by 40% in 2030. Furthermore, this global gap masks much more serious water gaps at the level of individual river basins. They estimate that one-third of the world's population in 2030 will live in basins where the projected gap is greater than 50 percent. In summary, it appears that water for agricultural irrigation will become much more expensive in the future – no doubt spurring considerable efficiency gains, but also raising the cost of production and sharply limiting the amount of land on which crops can be economically grown.

In addition to leading to an understatement of global area requirements, omitting explicit analysis of irrigation, and associated constraints, is likely to shift the distribution of land use changes towards dry (currently irrigated) regions with lower land use emission factors (less above-ground carbon). In the presence of irrigation constraints the distribution of land use changes induced by biofuel production will shift towards areas where expansion of rainfed agriculture is possible. These regions tend to be more carbon rich and therefore exhibit higher emissions factors. Hence, earlier models which ignore the role of irrigation in crop expansion tend to underestimate the ILUC emissions due to biofuel production. In this paper we explore the impact on ILUC emission estimates *if irrigated area cannot be expanded.* Since earlier studies have assumed the opposite (no constraint whatsoever on expansion), this paper offers an upper bound on the emission estimates of ILUC due to biofuel production. When combined with earlier estimates, this provides us with a useful set of outer bounds on ILUC related GHG emissions.

To accomplish this task, given the fact that a large-scale expansion in biofuels affects economic activities at a global scale, a Computational General Equilibrium (CGE) model is

developed based on a recent work of Taheripour, Hertel, and Tyner (2011). Those authors developed a global CGE model which handles production, consumption and trade of biofuels along with other economic activities, and which is capable of tracing the land use impacts of expansion in biofuels. Similar to most other models used for this purpose, Taheripour, Hertel, and Tyner (2011) ignores the role of irrigation. In this paper, we remedy this previous limitation.

We begin by modifying the GTAP database to distinguish irrigated and rainfed agriculture. Here we follow the pioneering work of Siebert and Döll (2010) who develop a land use data base which provides data on harvested area and crop production by 29 crops and 160 countries/regions at the 0.5x0.5 degree grid cell level. These spatially disaggregated data are aggregated to the level of 18 GTAP-AEZs, while maintaining the distinction between irrigated and rainfed crops. Using the information obtained from this data set, all crop industries presented in the v.6 GTAP database are broken into irrigated and rainfed categories.

In the second step, the GTAP-BIO-AEZ model used in Taheripour, Hertel and Taheripour (2011) is extended and modified to handle production, consumption and trade of irrigated and rainfed crops. To accomplish this task, all components of GTAP-BIO-AEZ model including: production, demand, and supply functions as well as market clearing conditions are revised. In this revised model, it is assumed that, for each crop, the irrigated and rainfed industries produce the same commodity (e.g. wheat) which enters the market and sells for the same price. This homogeneity assumption means that it is possible for irrigated production of any given crop to be completely eliminated if competition for irrigation is sufficiently intense in a given region.

This revised model is used to revisit the global land use impacts of biofuels expansion, comparing the findings to those previously obtained (ignoring potential irrigation constraints). In

order to establish an upper bound on changes due to the presence of irrigation, we assume that total irrigated area is fixed in each AEZ – although the crop to which the water is applied may be varied. Results show that the change in global cropland area is 15.8% larger when the irrigation constraint is imposed. This is a direct consequence of the lower yields in rainfed areas. The figure is larger in the US, where the elimination of potential for expanding irrigated areas results in 23% more cropland cover change. When combined with the altered geography of land use change in the irrigation constrained model, we obtain an estimate of land use related emissions equal to 36.7 grams/MJ of ethanol production in the presence of irrigation constraint. This figure is 21% higher than the corresponding figure obtained from a model with no irrigation constraint present.

In what follows we first review the literature of land use changes due to biofuel production. Then we explain construction of a new GTAP data base which we build to accomplish objective of this paper. After that we introduce modifications which we made in the GTAP-BIO-AEZ model to handle production of irrigated and rainfed crops. Then we define our simulation experiments and present the simulation results. The last section provides conclusions.

2. Literature review

Land use changes and their consequent emissions induced by crop expansion due to biofuel production are controversial issues. In recent years many papers have been published on this topic. The early papers suggested that biofuel production could have extraordinary land use implications (Searchinger et al. 2008, Fargione et al. 2008). The most recent papers on this topic indicate that the early estimates overstated the land use implications of biofuel production (Hertel et al., 2010, Taheripour et al., 2010, and Tyner et al., 2010). Figure 1 compares the early and most recent estimates for the ILUC due to US ethanol production. This figure indicates that

the most recent estimates for the ILUC are significantly lower than the earlier estimates. Searchinger et al. (2008) have provided the first peer-reviewed estimate for the ILUC (about 0.73 hectares of new cropland area per 1000 gallon of ethanol capacity). Those authors used a partial equilibrium modeling framework (FAPRI) to assess the ILUC due to US ethanol program. After that Hertel et al. (2010) using a general equilibrium model showed that full accounting for market mediated price responses to ethanol production, as well as the geography of world trade, contributed to significant reductions in estimated ILUC impacts. Those authors estimated that the ILUC for the US ethanol program is about 0.29 hectares per 1000 gallons of ethanol. In more recent work Taheripour, Hertel, and Tyner (2011) made several changes in the GTAP-BIO modeling framework and its data base and used the improved model to examine consequences of biofuel mandates for the global livestock industry. These authors projected that the US and EU biofuel mandates will jointly expand the global cropland area by 11.8 million hectares, but they have not evaluated the ILUC due to mandates of each region. In another line of research in this area Tyner et al. (2010) have extended the model developed in Taheripour, Hertel, and Tyner (2011) and provided three sets of estimates for the ILUC due to the US ethanol. As shown in Figure 1, the estimates provided by Tyner et al. (2010) are significantly lower than provided in Hertel et al. (2010). Several modifications such as incorporating cropland pasture into the GTAP land use data base, assigning higher productivity rates to new croplands (obtained from the Terrestrial Ecosystem Model (TEM)), and establishing a new baseline contributed to these further reductions.

Figure 1 also compares the estimates for the land use emissions due to US ethanol for the corresponding land use estimates. This figure also indicates that the most recent estimates for the land use emissions are significantly lower than the earlier estimates. The estimates for the land

use emissions due to US ethanol have followed a downward path from about 100 grams/MJ (estimated by Searchinger et al., 2008) to 14.5 grams/MJ (estimated by Tyner et al., 2010).

Despite the extensive work to date seeking to better understand the land use implications of biofuels, to date, no attempt has been made to examine the role of irrigation in biofuel-induced cropland expansion[1]. This paper expands the capability of the GTAP modeling framework which have been extensively used in land use assessments of biofuels, to disaggregate irrigation activities.[2]

3. Data base construction

In this paper we extend the GTAP-BIO-AEZ data base used in Taheripour et al. (2011) to incorporate crop industries by irrigation type. In so doing, we rely on the pioneering work done by Siebert and Döll (2010) who develop a data base which provides data on harvested area and yield by irrigation type for 29 groups of crops and 160 countries/regions at the 0.5x0.5 degree grid cell level. Henceforth we refer to this data set as S-D. We achieved this split through two steps which are explained in sequence below.

3.1 Determining harvested area and crop production by irrigation type

Based on the S-D data set we divided the harvested area and crop production of the SAGE/GTAP data base documented in Monfreda et al. (2008), into two categories of rainfed and irrigated (for details see Appendix A). The new database collapses all types of crops into 8 GTAP commodities and represents the harvested area and crop production by country, AEZ, and irrigation type.

[1] Some studies including Fraiture et al. (2008), Hoogeveen et al. (2009), and Dominguez-Faus et al. (2009) have examined water implications of producing biofuels at regional and global levels.

[2] In this paper we use the modeling framework developed in Taheripour, Hertel, and Tyner (2011) as our starting point. The model provided by these authors is not the latest version of GTAP-BIO, but it has almost all modifications which are confirmed through a peer-reviewing process.

Tables A2 and A3 of Appendix A summarize the new data set at an aggregated level which has only 19 regions. In this table we summed harvested areas and crops outputs over all types of crops and all AEZs. In this newly constructed data base, about 23% of the global harvested area is irrigated, while global irrigated lands account for about 38% of global agricultural outputs as measured in physical tons. This indicates that irrigated lands are more productive versus rainfed lands. The global average yields for irrigated and rainfed areas are about 10.8 mt/ha and 5.3 mt/ha.

To understand the role of irrigation in crop production, we review the new database from different angles. First, consider the geographical distributions of harvested area and crop production regardless of irrigation type. Table A2 shows that about 57% of global harvested areas belong to India (14.3%), China (12.6%), Sub Saharan Africa (10.7%), US (10.3%), and EU (9%) regions. Table A3 represents global distribution of crop production. This table indicates that the shares of India and Sub Saharan Africa in global crop production are about 9.5% and 4.4%, respectively. These figures are less than the shares of these regions in global harvested area. The share of China in global crop production is about 14.4%, moderately higher than its share in global harvested area. However, the shares of US and EU in global crop production are about 15% and 15.2% which are considerably higher than their shares in global harvested area. This indicates that the US and EU croplands are physically more productive compared to the world average productivity of land.

Now consider the global distributions of harvested area and crop production by irrigation type. Table A2 and Figure 2 indicate that about 60.3% of global rainfed harvested areas belong to Sub Saharan Africa (13.3%), India (11.6%), US (11.3%), EU (10.6%), and China (9%). Table A3 and Figure 3 show the global distribution of the rainfed crop production. They indicate that

the shares of Sub Saharan Africa and India in the rainfed crop production are respectively about 5.9% and 5.4%. These figures are significantly lower than their corresponding shares in the harvested rainfed areas. However, the shares of US and EU in the global rainfed crop production are about 16.2% and 20.5%, which are significantly larger than their shares in the global rainfed harvested areas. These figures indicate that productivities of the rainfed crops in these two regions (in particular in EU) are relatively higher than the world average.

Consider now the global distributions of harvested area and crop production for irrigated practices. Table A2 and Figure 2 show that more than 65% of the global irrigated areas belong to the Asian countries and regions, including such as China (24.6%), India (23.2%), and all countries located in South East Asia (18%). After these regions, the largest area of irrigated land belongs to the US which owns about 7.2% of the global irrigated areas. On the other hand, Table A3 and Figure 3 indicate that China, India, and US supply about 16%, 16%, and 13% of irrigated crops, respectively. These figures show that, while China and India control about half of the global irrigated areas, they account only for 32% the global irrigated crops.

We now use Figure 4 to analyze the harvested area and crop production within each region by irrigation type. The left panel of this figure indicates the shares of irrigated and rainfed harvested areas in each region. This panel indicates that agricultural activities in some regions like Canada, Russia, and Sub Saharan Africa are mainly relied on rainfed. On the other hand, counties located in Asia are relied more on irrigation.

The right panel on Figure 4 represents shares of irrigated and rainfed crops in each region. The share of irrigated crop is higher than the share of irrigated land in each region and all regions presented in Figure 4, except for Japan and China. This shows that in general irrigated areas are more productive than their counterpart rainfed areas in each region.

To investigate differences in yield by irrigation type consider Figure 5. This figure shows that irrigated croplands typically have much higher yields than their rainfed counterparts in each region. This figure shows that in Brazil there is a major difference between the yields of irrigated and rainfed lands. This is due to the fact that irrigated sugarcane provides much better yield than the rainfed. In preparing Figure 5 we summed up harvested areas and outputs over all types of crops and AEZ. To examine differences between the irrigated and rainfed yields by crops now consider Figure 6 which shows differences between the irrigated and rainfed yields for six crop categories for the major crop producer countries of US, EU, China, and India. This figure shows that in all of these counties irrigated and rainfed yields are different for each and every crop. It also indicates that yields are usually higher in US for almost all crops, with few exceptions. EU yields for the irrigated oilseeds and the rainfed wheat are higher than other regions. Among these 4 regions, India has the lowest yields for all 6 crop categories.

Figure 6 shows that the US rainfed and irrigated national yields are not very different for coarse grains. However, this is clearly a function of compositional effects, since, as Figure 7 shows, US rainfed and irrigated coarse grains at the AEZ level are very different. The largest differences between the rainfed and irrigated coarse grains yields arise in the drier AEZs, including AEZ7, AEZ8, AEZ13, AEZ14, which produce irrigated corn. However, in the Midwest areas where the rainfed corn is the dominant crop (mainly AEZ10 and AEZ11) there is no major difference between the irrigated and rainfed yields suggesting that irrigation in these regions is largely an occasional supplemental to normally ample rainfall.

3.2 Splitting GTAP database

The next step in constructing the irrigation-augmented model is to divide each and every crop activity in the GTAP data base into two crop industries representing irrigated and rainfed

production using the *SplitCom* program (Horridge, 2005). We established the split process based on the following assumptions. First, we assume that the irrigated and rainfed products are homogeneous. This means that the price of rainfed wheat and irrigated wheat are the same, and so on for other crops. Second, we assume that the rainfed and irrigated crop producers pay the same price for a given input. This means that, for example, the price of seed is the same for both producers. Third, we assume that the input-output ratio is the same for both rainfed and irrigated production. This means that the same amount of fertilizer is required to produce a ton of wheat, regardless of whether it is irrigated or rainfed. When combined with the equal output and input price assumptions, this implies that the cost shares are the same for each input used in the two industries. For example, the cost share of labor in the irrigated wheat industry must be the same as the cost share of labor in the rainfed wheat industry. Since the value of output per hectare will be higher on irrigated land (due to higher yields), and since the share of this higher value going to land is the same as for rainfed land, then the returns to irrigated land will also be higher.

These assumptions provide a theoretical basis for using *SplitCom* to divide each and every crop industry of GTAP into two distinct industries of irrigated and rainfed. The *SplitCom* program needs exogenous information on the shares of irrigated and rainfed industries in the sales, costs, and trade items of each crop industry to carry out the split process in each region (Horridge, 2005). To provide the required exogenous information, we calculated the shares of irrigated and rainfed quantities of production of each crop in total production of that crop. Then we run the *SplitCom* program sequentially to split each and every crop industry of GTAP into two distinct industries of irrigated and rainfed. Note that these procedures are made at the most disaggregated level of GTAP database and then we aggregate the results to the 19 region level used in this paper.

In the next stage we allocated the payments to the irrigated and rainfed croplands among the AEZs. In order to accommodate irrigation, we extended the AEZs as follows: the first 18 categories represent irrigated croplands and the second 18 groups represent rainfed croplands, giving a total of 36 AEZs in the irrigation-extended model. Note that in the new AEZ classification, AEZ1 and AEZ19 represent the standard definition of AEZ1, and so on for other AEZs. Table 1 represents the mapping of the new and old AEZs. This treatment of irrigated lands as separate land endowments means that total irrigated area will be deemed fixed for purposes of our analysis.

4. Modification in GTAP-BIO model

The standard GTAP modeling framework uses a one to one relationship between industries and commodities. This means that in the standard framework each industry produces only one commodity and each commodity is produced only by one industry. The GTAP-BIO modeling framework extended this tradition and considers production of two commodities by a single industry in order to handle biofuel by-products (Taheripour et al. 2010). In this paper we extend the GTAP-BIO model so that each crop could be produced by two different industries, one irrigated and one rainfed. In this model it is assumed that for each crop the irrigated and rainfed industries produce the same commodity (e.g. wheat) which enters the market and sells for the same price. This homogeneity assumption means that it is possible for irrigated production of any given crop to be completely eliminated if competition for irrigation is sufficiently intense in a given region. In particular, we introduce the following percentage change form equations into the model to handle production of one homogeneous commodity by two distinct industries:

$$pi_{irrigated_j} = pi_{rainfed_j} = ps_j, \ for\ all\ j \in set\ of\ crop\ commodities, \quad (1)$$

$$pi_j = \sum_{k \in top\_com}^{K} S_{jk} * pf_{jk} \;\; for\ all\ j \in crop\ industries\ set, \qquad (2)$$

$$qf_{jk} = qi_j - \varepsilon\left[pf_{jk} - pi_j\right] for\ all\ k \in top\_com\ set\ and\ all\ j \in crop\ industries\ set, \quad (3)$$

$$qo_c = \sum_{w \in irrigated, rainfed} supplyshr_{cw} * qi_w \;\; for\ all\ c \in crop\ commodity\ set. \qquad (4)$$

In the above equations *pi* and *qi* represent percent changes in the price and quantity of *j* at the industry level and *ps* and *qo* represent their corresponding percentage changes at the commodity market level (where there is no distinction made about method of production). The variables *qf* and *pf* stands for percentage changes in prices and quantities of inputs used for crop production at the industry level. Finally, S_{jk} represents the cost share of input *k* in industry *j*, ε is the elasticity of substitution among intermediate inputs, and $supplyshr_{cw}$ is the share of crop c supply by irrigation type *w*.

Equation (1) ensures that irrigated and rainfed industries which produce the same crop (e.g. wheat) will receive the same price and that the prices at the industry and commodity levels are the same. Equation (2) is the zero profit condition for each crop industry. Equation (3) represents the demand for intermediate input k in crop industry j, and finally equation (4) ensures market clearing condition for each crop.[3]

5. Experimental Design

To analyze the role of irrigation in determining the global land use consequences of biofuels we undertook two experiments. In the first experiment, following the existing literature in this field we ignored the irrigation constraint. We then simulate the land use consequences of an increase in US ethanol production from its 2001 level to 15 billion gallons, which is the

[3] In addition to the above changes we made the necessary changes in the GTAP code to support production of crops by irrigation type.

mandated level of ethanol for 2015. In the second experiment we made the same simulation while we assumed that irrigated areas are fixed and cannot be expanded in short run, either due to the lack of infrastructure or insufficient water. Nonetheless, in the second experiment we assume the allocation of irrigated land among its alternative uses within agriculture can vary due to the ethanol shock. This simulation establishes an upper bound on changes due to the presence of irrigation constraints. It represents an upper bound, since, in practice, we expect expansion of irrigation in some regions to be part of the global response to higher demand for agricultural products.

Following Hertel et al. (2010), in both experiments developed in this paper we only shocked US ethanol to isolate impacts of US ethanol production from other factors which shape the world economy.

6. Simulation results

6.1 Land use changes

Table 2 compares the regional land use changes obtained from the experiments with and without irrigation constraints. This table indicates that the models with and without irrigation constraints provide different pictures of the land use implications of ethanol production. Overall, the change in global cropland area is 15.8% larger when the irrigation constraint is imposed (i.e. 4,840.9 thousand hectares vs. 4,180.1 thousand hectares without the constraint). This is a direct consequence of the lower yields in rainfed areas. The difference is larger in the US, where the elimination of potential for expanding irrigated areas results in 23% more cropland cover change (i.e. 1,616.1 thousand hectares vs. 1,314.3 thousand hectares without the constraint).

The composition of land conversion also changes when we impose a constraint on irrigation expansion. Since rainfed agriculture is more likely than irrigated agriculture to compete with forest, the irrigation-enhanced model shows greater conversion of forest to cropland (up from 24% to 26.8% of total cropland conversion globally).

The results also show that the presence of potential irrigation constraints alters the geographic pattern of land use change in the wake of the US ethanol expansion. Table 3 indicates that the irrigation constraint expands land use changes due to US ethanol in some region such as Sub Saharan Africa and Middle East where rainfed croplands are infertile, and it has the opposite effect in regions such as China, Canada, and Japan where irrigation tends to occur in relatively lower productivity regions of the country.

Tables 2 and 3 show the overall land use impacts of the irrigation constraint at the national level. However, the picture at the AEZ level is more complex. To examine the impacts of irrigation constraint on the geographic pattern of land use with more details consider Table 4 which reports differences between the changes in cropland areas obtained from the model with and without water constraint for some selected regions including US, EU, Brazil, China, and India by AEZ. In this table positive numbers indicate more cropland cover expansion in a given region in the presence of the irrigation constraint, while negative numbers indicate a reduction in cropland cover change when the irrigation constraint is imposed. This table shows that US AEZ7 and AEZ13 show reductions in cropland expansion of -77812 and -2529 hectares. These two AEZs heavily rely on irrigation in crop production, and the constraint that irrigation cannot be expanded limits the potential for expanding cropland cover in these AEZs. Meanwhile, with grazing and forestry areas being contracted in other AEZs, there is some incentive for them to expand in these AEZs with lower rainfed crop productivity.

Table 4 reports increases in cropland expansion for those AEZs in the US where irrigation does not play a significant role. For example, this table indicates that in AEZ9, AEZ10, and AEZ11 ethanol-induced cropland expansion increases by 39008, 168140, and 91382 hectares in the presence of the irrigation constraint. The movement of cropland cover changes from irrigated to rainfed areas can be observed in other countries as well. However, in regions such as China where the shares of irrigated and rainfed cropping activities are not very different in most of the AEZs, it is not easy to trace the movement of cropland cover changes from irrigated to rainfed areas.

Map 1 also reports the change in cropland cover across the world owing to increased ethanol production in the US once the irrigation constraint is imposed globally. In this map positive numbers indicate more cropland cover expansion in a given region, due to the irrigation constraint, while negative numbers indicate a reduction in cropland cover change when the irrigation constraint is imposed. Not surprisingly, US cropland cover change is shifted to the area east of the Mississippi River when potential irrigation limitations are taken into account. In Africa, there is a sharp contrast between the land cover changes in North Africa (negative to zero) and those in Sub-Saharan Africa (positive).

6.2 Land use emissions

To calculate land use emissions due to US ethanol production for the cases with and without irrigation constraint we rely on the land use emissions factors reported in Tyner et al. (2010). The land use emissions calculated for the two simulation results are shown in table 5. This table indicates that increasing US ethanol production from its 2001 level to 15 billion gallons causes about 2436 grams CO2 equivalent per gallon of ethanol (about 30.2 grams/MJ), if we ignore the role of irrigation constraint. Adding this constraint into the model increases the

land emissions to 2956 grams per gallon of ethanol (about 36.7 grams/MJ). This means that the change in GHG emissions is 21.3% larger when the irrigation constraint is imposed. This stems both from greater cropland expansion overall, as well as from the tendency to convert more forest per hectare of cropland. About 74% of the additional emissions are due to cropland expansion and the rest is due to changes in the composition of global land use.

7. Conclusions

In recent years numerous studies have examined the global land use changes and consequent emissions due to biofuel expansion across the world. These studies have effectively considered all croplands as being rainfed; thereby ignoring the role of irrigation in biofuel-induced land use changes. This paper develops a new general equilibrium framework which disaggregates irrigated and rainfed cropping industries to examine the role of potential irrigation constraints in biofuel induced land use changes. This study shows that models which ignore the role irrigation tend to systematically underestimate the induced land use changes due to US ethanol program. The ensuing estimates of land use change provide an upper bound for the land use change due to US ethanol production, if irrigated cropland cannot be expanded either due to the lack of infrastructure or limits on water for irrigation. The paper indicates that change in global cropland area is 15.8 % larger when the irrigation constraint is imposed. This leads to 21.3% increase in land use emissions due to US ethanol production. The true answer surely lies between this upper bound estimate and existing estimates which ignore the role of irrigation altogether. Future research in this area needs to explicitly model the potential for irrigation expansion on a global scale.

References

- Cai, X., and M. Rosegrant, (2002), "Global water demand and supply projections*:* Part 1: A modeling approach", *Water International*, 27(2): 159-169.
- Dominguez-Faus, R., S. Powers, J. Burken, and J. Alverez, (2009). "The water footprint of biofuels: A drink or drive issue", *Environmental Science and Technology*, Vol. 43 (9): 3005-3010.
- Fargione, J., J. Hill, D. Tilman, S. Polasky, and P. Hawthorne, (2008). "Land clearing and the biofuel carbon debt" Science 319:1235–1238.
- Fraiture , C., M. Giordano, and Y. Liao, (2008). "Biofuels and implications for agricultural water use: blue impacts of green energy", *Water Policy 10 Supplement 1*: 67–81.
- Gurgel, A., J. Reilly, S. Paltsev, (2007). "Potential land use implications of a global biofuels industry," *Journal of Agricultural and Food Industrial Organization* 5: Article 9.
- Hertel, T., A. Golub, A. Jones, M. O'Hare, R. Pelvin, and D. Kammen, (2010). "Effects of U.S. maize ethanol on global land use and greenhouse gas emissions: Estimating market-mediated responses." *BioScience Vol. 60 No. 3*: 223- 231.
- Hoogeveen, J., J. Faures, and N. Giessen, (2009). "Increased biofuel production in the coming decade: To what Extend will it affect global Freshwater resources", *Irrigation and Drainage* 58: 148-160.
- Horridge M., (2005). "SplitCom - programs to disaggregate a GTAP sector." Centre of Policy Studies, Monash University, Melbourne, Australia.
- McKinsey & Co, (2009). "Charting our water future", Economic frameworks to inform decision-making, 2030 Water Resources Group.

- Monfreda, C., N. Ramankutty, and J. Foley, (2008). “Farming the planet: 2. Geographic distribution of crop areas, yields, physiological types, and net primary production in the year 2000”, *Global Biogeochemical Cycles*, *22*, GB1022.
- Searchinger, T., R. Heimlich, R. Houghton , F. Dong, A. Elobeid, J. Fabiosa, S. Tokgoz , D. Hayes, T. Yu, (2008). “Use of U.S. croplands for biofuels increases greenhouse gases through emissions from land use change.” *Science* 319:1238-1240.
- Siebert, S. and P. Döll, (2010). “Quantifying blue and green virtual water contents in global crop production as well as potential production losses without irrigation”. *Journal of Hydrology* 384, no. 3-4 (April 30): 198-217.
- Taheripour, F., T. Hertel, and W. Tyner, (2011). “Implications of biofuels mandates for the global livestock industry: a computable general equilibrium analysis” *Agricultural Economics*, 42:325-242.
- Taheripour, F., T. Hertel, W. Tyner, J. Bechman, and D. Birur, (2010). “Biofuels and their by-products: Global economic and environmental implications”, *Biomass and Bioenergy*, 2010. 34: 278-89.
- Tyner, W., F. Taheripour, Q. Zhuang, D. Birur, and U. Baldos, (2010). “Land Use Changes and Consequent CO2 Emissions due to US Corn Ethanol Production: A Comprehensive Analysis”, A Report to Argonne National Laboratory, Department of Agricultural Economics, Purdue University.

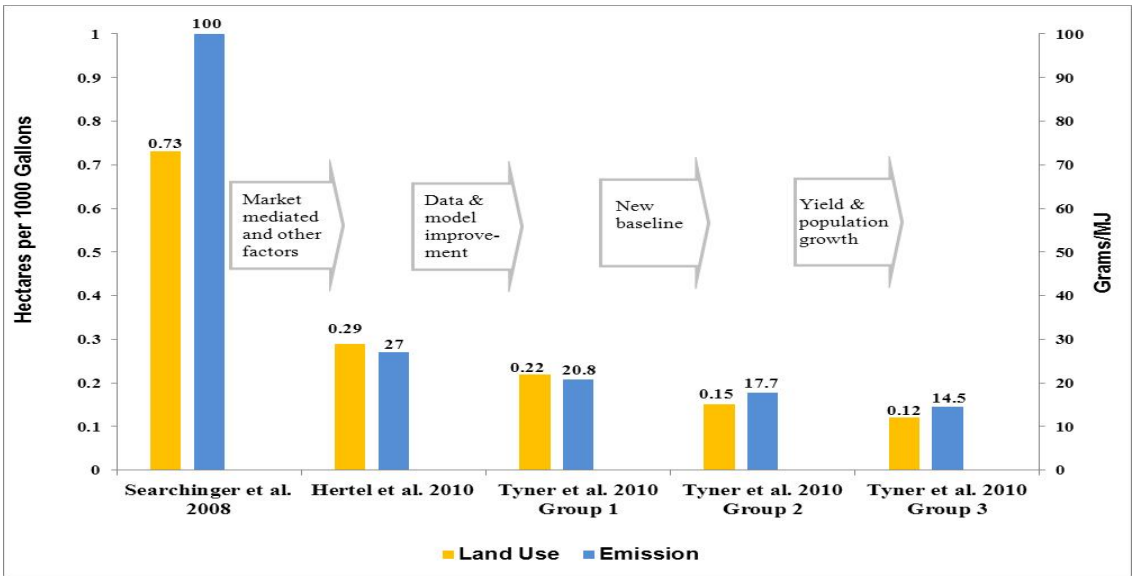

Figure 1. Estimates for additional land requirement and land use emissions due to US ethanol production

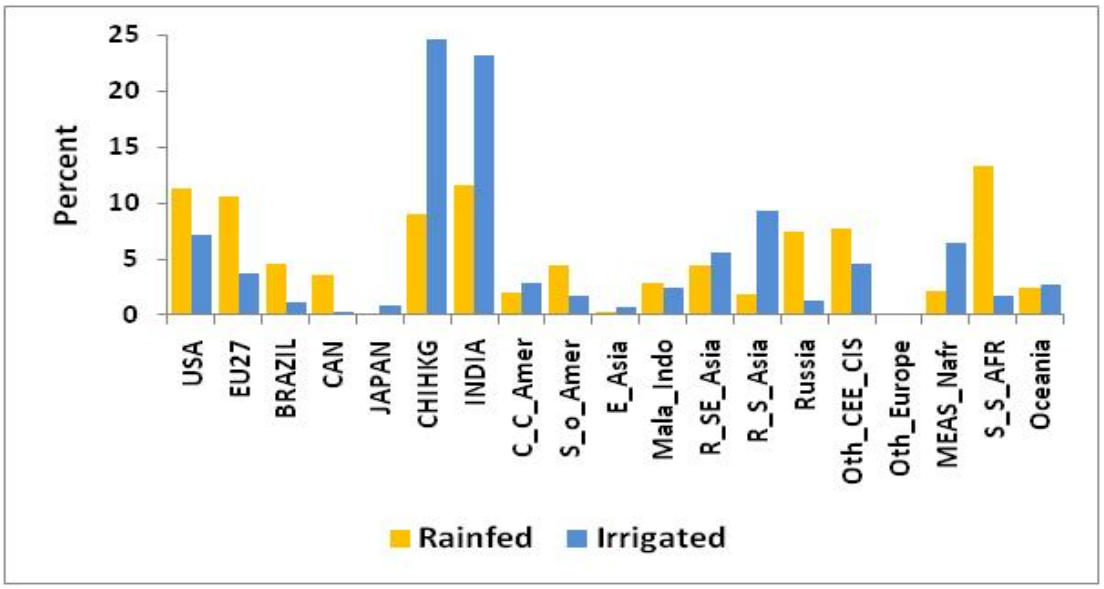

Figure 2. Global distribution of harvested area by irrigation type

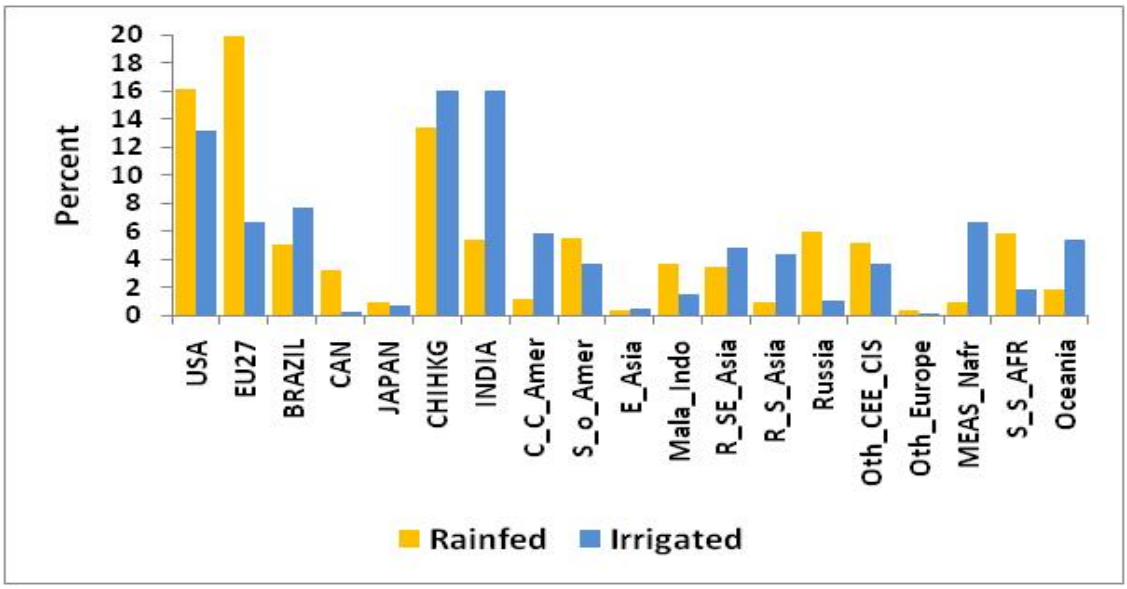

Figure 3. Global distribution of crop production by irrigation type

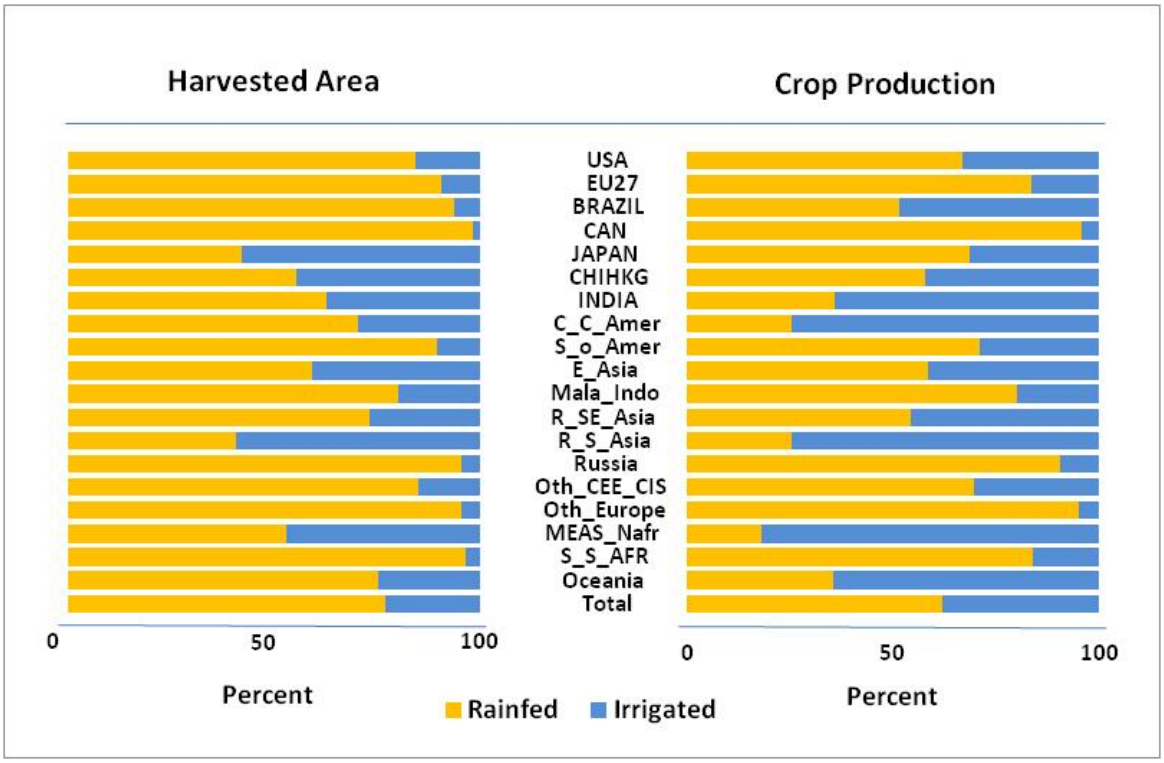

Figure 4. Harvested areas and crop production by region and by irrigation type

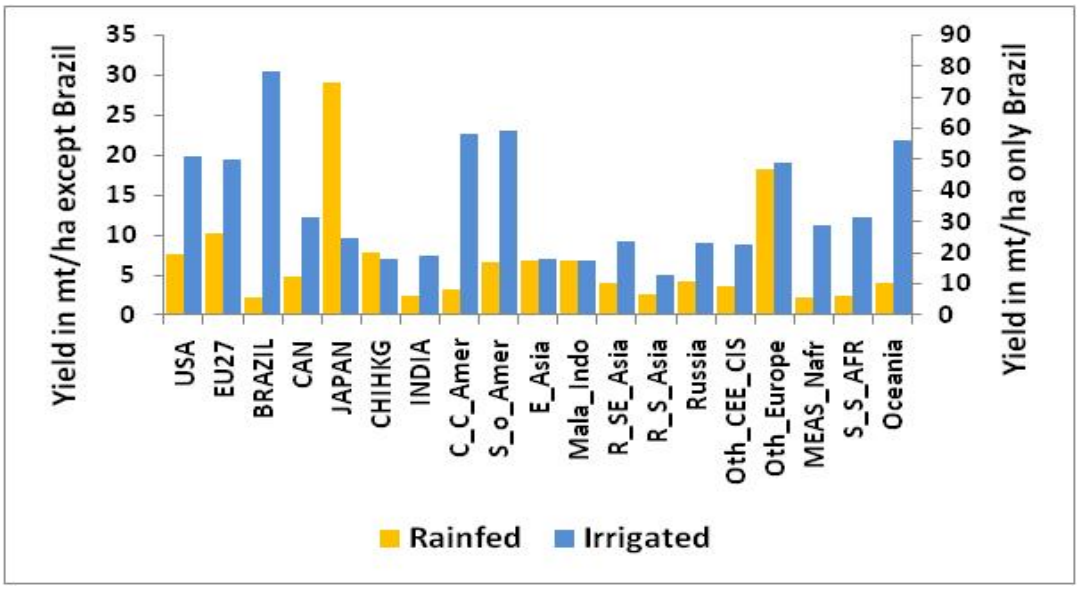

Figure 5. Irrigated and rainfed yields by region

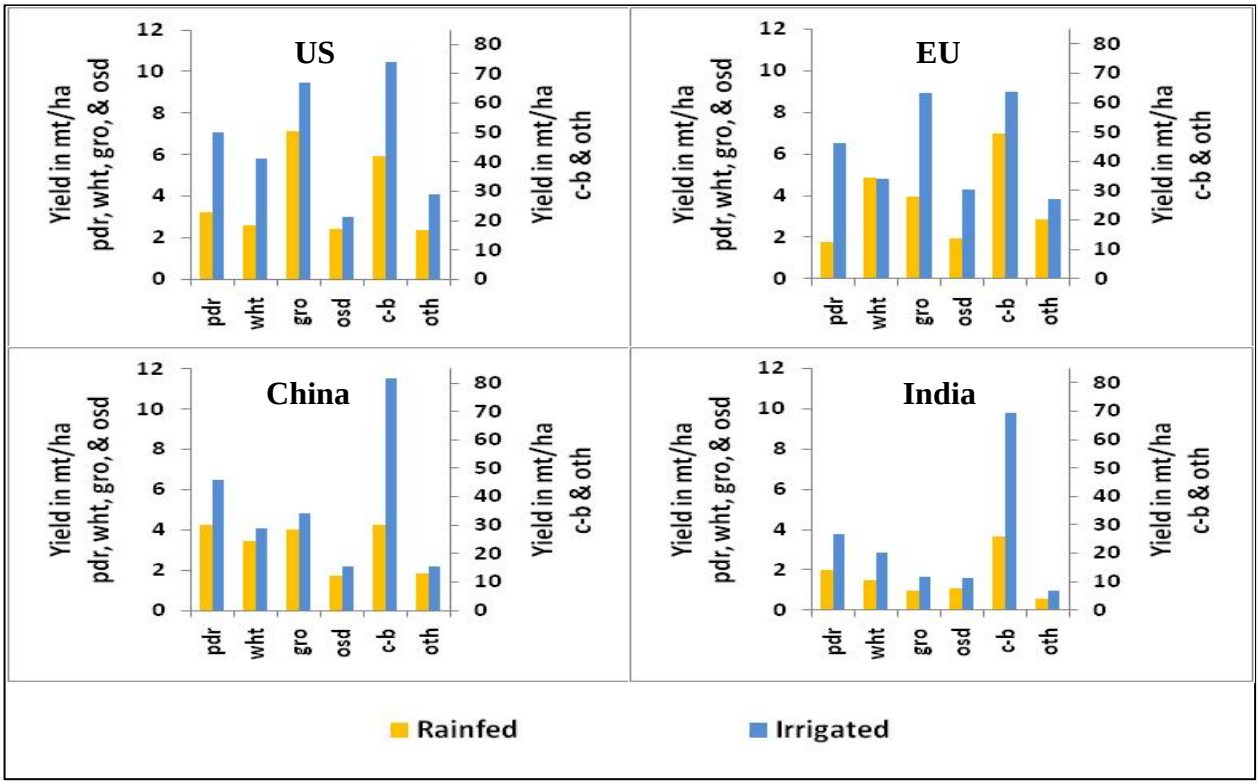

Figure 6. Irrigated and rainfed yields by crop types for selected regions

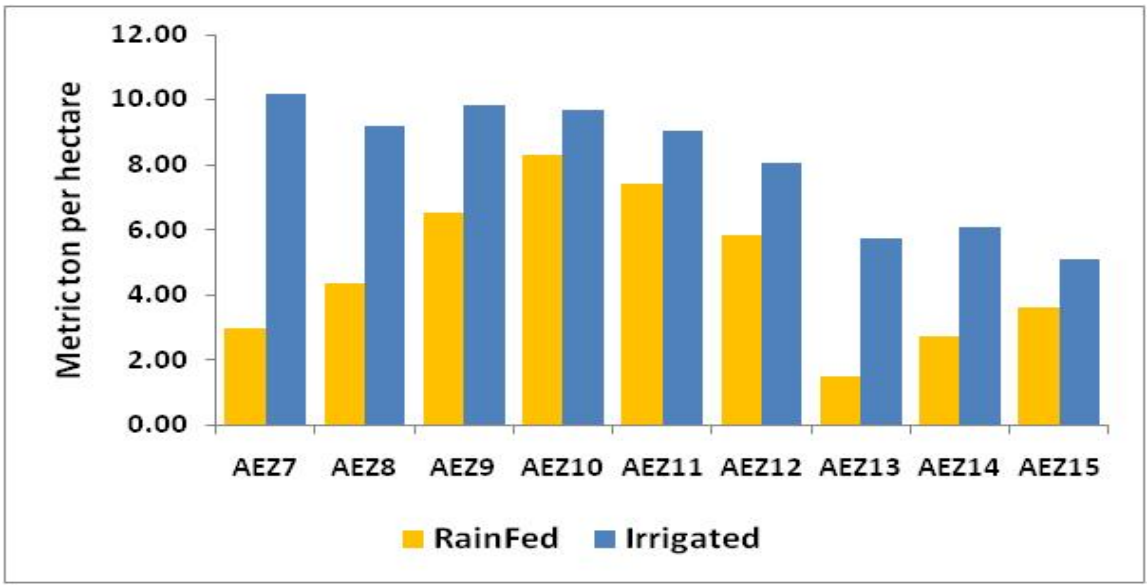

Figure 7. US coarse grains yields by irrigation type and AEZ

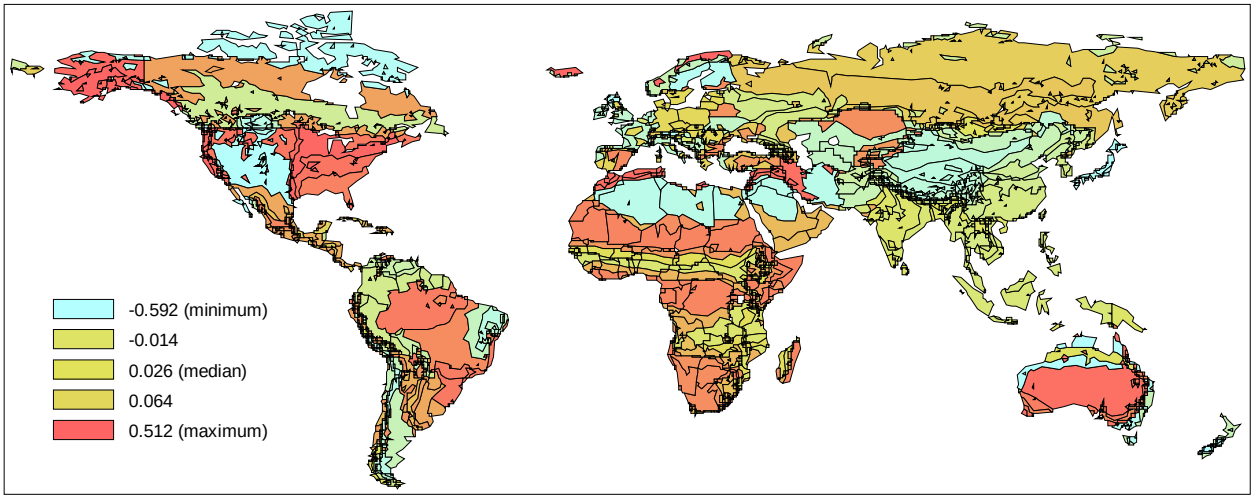

Map 1. Cropland cover changes due to irrigation Constraint*

* Figures used this map are: %change in crop cover obtained from the model with irrigation constraint minus the corresponding figure from the model with no irrigation constraint.

Table 1. Mapping of the new and standard AEZs

New Irrigated AEZ	New Rainfed AEZs	Standard AEZ
1	19	1
2	20	2
3	21	3
4	22	4
5	23	5
6	24	6
7	25	7
8	26	8
9	27	9
10	28	10
11	29	11
12	30	12
13	31	13
14	32	14
15	33	15
16	34	16
17	35	17
18	36	18

Table 2. Land use changes due to US ethanol production (1000 hectares)

Region	Model without irrigation constraint			Model with irrigation constraint		
	Cropland	Forestry	Pastureland	Cropland	Forestry	Pastureland
USA	1314.3	-519.5	-794.8	1616.1	-711.3	-904.8
EU27	423.2	-274.9	-148.3	431.9	-280.9	-151.0
BRAZIL	291.3	-72.4	-218.9	341.0	-102.4	-238.6
CAN	434.1	-259.8	-174.3	432.8	-272.9	-159.9
JAPAN	10.2	-8.5	-1.7	3.1	-1.4	-1.7
CHIHKG	53.7	61.1	-114.8	33.3	57.3	-90.7
INDIA	80.9	-39.5	-41.4	96.3	-48.5	-47.9
C_C_Amer	95.8	-24.5	-71.3	121.4	-36.8	-84.6
S_o_Amer	150.6	79.4	-230.0	173.7	70.9	-244.6
E_Asia	1.8	9.2	-11.0	2.2	8.5	-10.8
Mala_Indo	-2.0	9.2	-7.1	2.6	4.4	-7.0
R_SE_Asia	4.2	3.9	-8.1	6.5	1.2	-7.6
R_S_Asia	26.0	-7.5	-18.5	22.2	-8.0	-14.2
Russia	-13.4	243.5	-230.1	-0.4	225.2	-224.9
Oth_CEE_CIS	196.4	-23.0	-173.5	220.3	-13.2	-207.1
Oth_Europe	5.9	-3.3	-2.6	6.0	-3.5	-2.6
MEAS_NAfr	100.3	0.5	-100.8	189.5	-0.3	-189.2
S_S_AFR	884.9	-175.4	-709.5	984.7	-179.3	-805.5
Oceania	121.8	-3.8	-117.9	157.6	-4.0	-153.6
TOTAL	4180.1	-1005.4	-3174.7	4840.9	-1294.8	-3546.1

Table 3. Differences in land use changes obtained from models with and without irrigation constraint (1000 hectares)

Region	Cropland	Forest	Pastureland
USA	301.8	-191.8	-110.0
EU27	8.7	-6.0	-2.7
BRAZIL	49.7	-29.9	-19.7
CAN	-1.3	-13.1	14.5
JAPAN	-7.1	7.1	0.0
CHIHKG	-20.3	-3.8	24.1
INDIA	15.4	-9.0	-6.4
C_C_Amer	25.6	-12.3	-13.3
S_o_Amer	23.1	-8.4	-14.6
E_Asia	0.4	-0.6	0.2
Mala_Indo	4.7	-4.8	0.1
R_SE_Asia	2.3	-2.7	0.4
R_S_Asia	-3.8	-0.5	4.3
Russia	13.0	-18.3	5.2
Oth_CEE_CIS	23.8	9.8	-33.6
Oth_Europe	0.1	-0.2	0.1
MEAS_Nafr	89.3	-0.9	-88.4
S_S_AFR	99.8	-3.9	-95.9
Oceania	35.9	-0.2	-35.7
Total	660.8	-289.4	-371.5

Table 4. Differences in cropland changes obtained from models with and without irrigation constraint for some selected countries (hectares)

AEZ/Region	US	EU	Brazil	China	India
AEZ1	0	0	-43	0	1321
AEZ2	0	0	-439	0	1609
AEZ3	0	0	-5767	0	6744
AEZ4	0	32	-2436	0	2456
AEZ5	0	0	14586	-7	1301
AEZ6	0	0	16217	339	301
AEZ7	-77812	0	0	-5334	1052
AEZ8	63366	776	0	-6287	1633
AEZ9	39008	17260	0	-2662	959
AEZ10	168140	19185	173	-2194	-1556
AEZ11	91382	-20229	-6	-1320	-216
AEZ12	19121	-4413	27379	1004	-177
AEZ13	-2529	-1	0	-1411	-2
AEZ14	1059	-22	0	-674	-6
AEZ15	94	-2931	0	-1478	-23
AEZ16	9	-931	0	-294	-19
AEZ17	0	0	0	-23	0
AEZ18	0	0	0	0	0
Total	301836	8725	49664	-20339	15377

Table 5. Land use emissions due to US ethanol production

Simulations	Biofuel Production BG	Annual LUC Emissions (million metric ton CO_2 equivalent)			Annual LUC Emissions (grams of CO2 equivalent per gallon of fuel)		
		Forest	Grassland	Total	Forest	Grassland	Total
Model without irrigation constraint	13.23	17.83	11.97	29.79	1458	978	2436
Model with irrigation constraint	13.23	23.23	12.92	36.15	1899	1057	2956

Appendix A

Harvested area and crop production by irrigation type

In this appendix, we explain the process we followed to split the SAGE data set on harvested area and crop production documented in Monfreda et al. (2009) into irrigated and rainfed categories. To achieve this goal we used Siebert and Döll (2010) data on harvested area and yield by irrigation type. Henceforth we refer to their data set as S-D. This data set classifies global harvested area for 29 crop categories at 0.5^{o} x 0.5^{o} spatial resolution by irrigation type. It also provides information on crop yields by irrigation type for the 29 crop categories at the same spatial resolution.

We began with the S-D data at the grid cell level. Given the harvested area and yield by irrigation type we used the following relationship to calculate gridded crop production by irrigation type for the 29 crop categories:

$$Q_{ij}^{w} = A_{ij}^{w} \cdot Y_{ij}^{w}$$

Here *Q*, *A*, and *Y* represent crop quantity, harvested area, and yield. The superscript *w* denotes irrigation type with: with either *w* = irrigated or *w* = rainfed, *i* indicates crop type with 29 members based on S-D, and *j* shows the index of grid cell for all grid cells available in S-D data set.

We then matched S-D grid cells with the GTAP-AEZ profile at the grid cell to aggregate harvested areas and quantities of crops up to country by AEZ level. The mapping schedule presented in Table A1 was then used to match the S-D 29 crop categories with SAGE crop categories aggregated to 8 crop categories which we use in GTAP database. Using this mapping schedule we aggregated the S-D data set to the 8 SAGE /GTAP crop categories. Then we used the following relationships to split harvested area and crop production of SAGE/GTAP data into irrigated and rainfed categories:

$$Q_{irz}^{w^{SAGE}} = \left[\frac{Q_{irz}^{w^{S-D}}}{\sum_w Q_{irz}^{w^{S-D}}}\right] \cdot Q_{irz}^{SAGE}$$

$$A_{irz}^{w^{SAGE}} = \left[\frac{A_{irz}^{w^{S-D}}}{\sum_w A_{irz}^{w^{S-D}}}\right] \cdot A_{irz}^{SAGE}$$

These two equations serve to 'share out' quantity produced and area harvested in the SAGE data base into irrigated and rainfed components. Specifically, *Q* and *A* represent crop quantity and harvested area, *w* shows the index of irrigation type with two categories of irrigated and rainfed, *i* indicates crop type with 8 members, and *r* shows the index of region for all region in the data set, *z* is the index of AEZ from 1 to 18, and finally *S-D* and *SAGE* represent their corresponding data sets.

Finally, the results obtained from the above step are aggregated to the 19 model regions which we use in this paper. Tables A2 and A3 report the results of this splitting process for harvested areas and crop production by irrigation type by the 19 regions which we use in this paper.

Table A1. S-D and SAGE crop categories

S-D crop categories	GTAP/SAGE crop categories	S-D crop categories	GTAP/SAGE crop categories
Wheat	wht	Groundnuts / Peanuts	osd
Maize for grain	gro	Pulses	v-f
Rice	pdr	Citrus	v-f
Barley	gro	Date palm	v-f
Rye for grain	gro	Grapes / vine	v-f
Millet	gro	Cotton	pfb
Sorghum for grain	gro	Cocoa	ocr
Soybeans	osd	Coffee	ocr
Sunflower	osd	Others perennial	ocr
Potatoes	v-f	Managed grassland/pasture	ocr
Cassava	v-f	Others annual	ocr
Sugar cane	c-b	Maize, forage	ocr
Sugar beets	c-b	Rye, forage	ocr
Oil palm	osd	Sorghum, forage	ocr
Rapeseed / canola	osd		

Table A2. Geographical distribution of land by irrigation type

Region	Area (million hectares)			Distribution by irrigation (%)			Geographical distribution (%)		
	Rainfed	Irrigated	Total	Rainfed	Irrigated	Total	Rainfed	Irrigated	Total
USA	111.1	21.0	132.0	84.1	15.9	100.0	11.3	7.2	10.3
EU27	104.2	10.8	115.0	90.6	9.4	100.0	10.6	3.7	9.0
BRAZIL	45.4	3.1	48.5	93.5	6.5	100.0	4.6	1.1	3.8
CAN	34.7	0.6	35.3	98.3	1.7	100.0	3.5	0.2	2.8
JAPAN	1.8	2.4	4.2	42.0	58.0	100.0	0.2	0.8	0.3
CHIHKG	88.8	72.1	160.9	55.2	44.8	100.0	9.0	24.6	12.6
INDIA	114.2	68.0	182.2	62.7	37.3	100.0	11.6	23.2	14.3
C_C_Amer	19.4	8.2	27.6	70.1	29.9	100.0	2.0	2.8	2.2
S_o_Amer	43.5	5.1	48.6	89.4	10.6	100.0	4.4	1.8	3.8
E_Asia	3.0	2.1	5.0	59.1	40.9	100.0	0.3	0.7	0.4
Mala_Indo	28.5	7.1	35.6	80.0	20.0	100.0	2.9	2.4	2.8
R_SE_Asia	44.2	16.4	60.6	73.0	27.0	100.0	4.5	5.6	4.7
R_S_Asia	18.7	27.1	45.8	40.8	59.2	100.0	1.9	9.2	3.6
Russia	72.9	3.6	76.5	95.3	4.7	100.0	7.4	1.2	6.0
Oth_CEE_CIS	75.3	13.6	88.9	84.8	15.2	100.0	7.7	4.6	7.0
Oth_Europe	1.0	0.1	1.1	95.3	4.7	100.0	0.1	0.0	0.1
MEAS_Nafr	21.1	18.9	40.0	52.7	47.3	100.0	2.1	6.5	3.1
S_S_AFR	131.0	4.9	135.9	96.4	3.6	100.0	13.3	1.7	10.7
Oceania	24.2	8.0	32.1	75.2	24.8	100.0	2.5	2.7	2.5
Total	982.8	293.1	1275.9	77.0	23.0	100.0	100.0	100.0	100.0

Table A3. Geographical distribution of crop production by irrigation type

Region	Production (million metric tons)			Distribution by irrigation (%)			Geographical distribution (%)		
	Rainfed	Irrigated	Total	Rainfed	Irrigated	Total	Rainfed	Irrigated	Total
USA	839.7	417.2	1256.8	66.8	33.2	100.0	16.2	13.1	15.0
EU27	1064.5	210.9	1275.3	83.5	16.5	100.0	20.5	6.6	15.2
BRAZIL	261.1	245.0	506.1	51.6	48.4	100.0	5.0	7.7	6.0
CAN	165.0	7.5	172.5	95.7	4.3	100.0	3.2	0.2	2.1
JAPAN	50.9	23.4	74.3	68.5	31.5	100.0	1.0	0.7	0.9
CHIHKG	696.4	507.8	1204.1	57.8	42.2	100.0	13.4	16.0	14.4
INDIA	283.4	509.3	792.7	35.7	64.3	100.0	5.5	16.0	9.5
C_C_Amer	63.2	186.6	249.7	25.3	74.7	100.0	1.2	5.9	3.0
S_o_Amer	286.6	118.0	404.6	70.8	29.2	100.0	5.5	3.7	4.8
E_Asia	20.5	14.5	34.9	58.6	41.4	100.0	0.4	0.5	0.4
Mala_Indo	191.1	48.0	239.1	79.9	20.1	100.0	3.7	1.5	2.9
R_SE_Asia	179.4	151.6	331.0	54.2	45.8	100.0	3.5	4.8	4.0
R_S_Asia	46.8	137.6	184.5	25.4	74.6	100.0	0.9	4.3	2.2
Russia	310.2	32.8	343.0	90.4	9.6	100.0	6.0	1.0	4.1
Oth_CEE_CIS	268.5	118.1	386.6	69.5	30.5	100.0	5.2	3.7	4.6
Oth_Europe	18.7	1.0	19.7	95.0	5.0	100.0	0.4	0.0	0.2
MEAS_Nafr	47.2	212.7	259.8	18.1	81.9	100.0	0.9	6.7	3.1
S_S_AFR	305.4	59.5	365.0	83.7	16.3	100.0	5.9	1.9	4.4
Oceania	94.6	173.3	267.9	35.3	64.7	100.0	1.8	5.5	3.2
Total	5193.0	3174.6	8367.6	62.1	37.9	100.0	100.0	100.0	100.0